

TGS: Trajectory Generation and Selection using Vision Language Models in Mapless Outdoor Environments

Daeun Song^{1*}, Jing Liang^{1*}, Xuesu Xiao², and Dinesh Manocha¹

¹ University of Maryland

² George Mason University

Abstract. We present a multi-modal trajectory generation and selection algorithm for real-world mapless outdoor navigation in challenging scenarios with unstructured off-road features like buildings, grass, and curbs. Our goal is to compute suitable trajectories that (1) satisfy the environment-specific traversability constraints and (2) generate human-like paths while navigating in crosswalks, sidewalks, etc. Our formulation uses a Conditional Variational Autoencoder (CVAE) generative model enhanced with traversability constraints to generate multiple candidate trajectories for global navigation. We use VLMs and a visual prompting approach with their zero-shot ability of semantic understanding and logical reasoning to choose the best trajectory given the contextual information about the task. We evaluate our methods in various outdoor scenes with wheeled robots and compare the performance with other global navigation algorithms. In practice, we observe at least 3.35% improvement in the traversability and 20.61% improvement in terms of human-like navigation in generated trajectories in challenging outdoor navigation scenarios.

Keywords: Motion Planning, AI-enabled Robotics, Algorithms for Robotics

1 Introduction

Mapless navigation is used to compute trajectories or directions for robots to navigate in large-scale environments without relying on accurate maps [14, 35]. This problem is important for outdoor global navigation. Unlike map-based methods [12, 13, 30], which require an accurate and extensive global map, mapless approaches [22, 24, 35] do not need to maintain an accurate map and are capable of adapting to frequently changing environments [43], including weather changes [29, 48], temporary construction sites [19], and hazardous areas [9]. However, mapless global navigation can be challenging due to traversability analysis and scene understanding in terms of navigation and social protocols [14, 35].

Traditional mapping-based approaches [8, 10] and learning-based methods [22, 23, 37, 41] often rely on properties such as elevations to analyze traversability.

*Equal contribution.

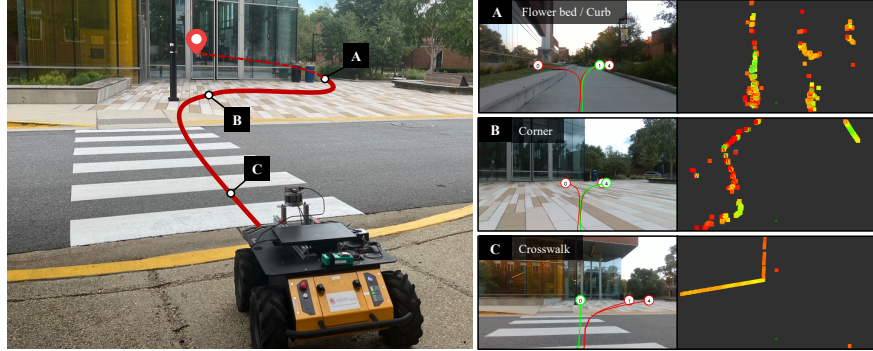


Fig. 1. Long-range navigation trajectories generated and selected using TGS. The example path includes three different types of scenarios: (A) flower bed and curb, (B) corner, and (C) crosswalk. On the left, the map pin icon marks the goal behind the building, with the red solid or dashed line highlighting the robot’s path. The red dashed line represents the trajectory behind the building. On the right, we show the visually marked candidate trajectories in red lines with numbers. The green path corresponds to the trajectory computed using TGS. Overall, TGS is capable of generating diverse, geometrically traversable paths and selecting human-like trajectories for navigation.

However, these properties may not be applicable to all types of robots, for example, stairs can be traversed by legged robots, but not by wheeled robots [10, 41]. To address these challenges, multi-modal sensors can be used for better scene understanding. Specifically, LiDAR sensors provide geometric information about the environment and can be used for handling collisions [23, 25]. However, it is difficult to use a LiDAR to detect terrains with different colors but similar geometric properties, such as elevations [22]. RGB cameras can be used to provide color and semantic information for scene understanding [21, 31, 34, 44].

Scene understanding is important for outdoor navigation, enabling robots to make human-like decisions by following social protocols and identifying efficient paths. It is challenging because the required information varies significantly across different environments. For instance, off-road navigation requires an understanding of unstructured vegetation to determine whether the robot can traverse it [26, 42]. On the other hand, social navigation tasks [15, 40] require recognizing social cues. Consequently, it is useful to have a general-purpose scene understanding method in terms of traversability for specific types of robots, social interactions, and identifying directions that could lead to dead-ends. Many current methods [20, 42, 47] rely on segmentation or classification [6, 21], but these require extensive training with ground truth data and are limited to the labeled datasets. This limitation hinders their generalizability to scenarios with complex terrain and social constraints. Recent advances in Large Language Models (LLMs) and Vision Language Models (VLMs) have demonstrated strong capabilities across a wide range of tasks, including logical reasoning [4, 7, 16] and visual understanding [2, 31]. VLMs, in particular, have the ability to process and understand both visual and textual information, which enables them to perform

a wide range of multi-modal tasks. Recently, VLMs have been used to navigate robots autonomously in outdoor scenarios by understanding the surrounding environment through images and contextual cues [11, 18, 36]. However, a notable challenge is that VLMs cannot directly provide precise spatial geometric outputs [36, 40].

Main Results: We present TGS, a novel multi-modal approach for trajectory generation and selection in mapless outdoor navigation. Our method leverages both RGB color and LiDAR geometric information for traversability analysis. We use a model-based trajectory generation to generate multiple candidate trajectories based on the LiDAR scene perception. We also use VLMs for scene understanding based on RGB color data. Although VLMs cannot provide precise spatial outputs, we use visual annotations to aid in selecting among a discrete set of coarse choices [28, 38, 45]. We use VLMs to make human-like decisions to choose suitable trajectories among the candidates for global navigation that satisfy the traversability constraints. We demonstrate the effectiveness of our approach in complex outdoor scenarios that include diverse unstructured environments and navigation constraints, such as such as crossing streets at crosswalks and maneuvering around buildings. The major contributions of our work include:

1. A novel integrated trajectory generation and selection method, TGS to generate multiple candidate trajectories using a CVAE-based [39] approach and to select the most suitable trajectory using VLMs with a visual prompting approach. Our CVAE-based trajectory generation method generates multiple candidate trajectories that are traversable considering the geometrical information retrieved from the LiDAR sensor. Our VLM-based trajectory selection method selects the best trajectory, which is traversable, in terms of both geometric and semantic manner, and closest to the target.
2. We explore the use of a visual prompting approach to enhance the spatial reasoning capabilities of VLMs in the context of trajectory selection. By incorporating visual markers such as lines and numerical indicators within the RGB image, we provide explicit guidance to the VLMs. It helps to bridge the gap between the concrete geometric information from LiDAR data and the contextual understanding provided by VLMs.
3. We evaluate TGS in four different challenging outdoor scenarios. We measure the traversability rate and the Fréchet distance with respect to a human-generated trajectory. We compare the results with the state-of-the-art trajectory generation approaches, ViNT [37], NoMaD [41], MTG [22], and CoN-VOI [32]. We observe at least 3.35% improvement in traversability and 20.61% improvement in the Fréchet distance. We also qualitatively demonstrate the benefits of our approach over other methods.

2 Related Work

In this section, we review the related works on outdoor robot navigation, especially focusing on trajectory generation.

Outdoor Mapless Global Navigation: Reinforcement-learning-based motion planning approaches [17, 23] use an end-to-end structure to take observations and generate actions or trajectories. However, these methods are designed for short-range navigation, and on-policy reinforcement learning approaches also suffer from the reality gap. Map reconstruction with path planning approaches [33, 46] provides a solution for global planning by building a map during navigation, but these approaches require large memory for the global map. To address this issue, NoMaD [41] and ViNT [37] use topological maps to reduce memory usage for navigation, but these approaches require topological nodes to be predefined, making them unsuitable for fully unknown environments. To overcome these limitations, our approach uses CVAE-based trajectory generation method [22] to generate long trajectories and leverages VLMs to select the optimal trajectory to reach the goal.

Traversability Analysis: Some approaches build local maps for traversability analysis [8, 10], but these methods require significant computational resources [10], and the maps still need to be combined with motion planning algorithms to generate motions or trajectories. Learning-based approaches offer an end-to-end solution for traversability analysis by directly generating trajectories [22–24, 37, 41]. However, these methods generate trajectories based on specific robot properties, such as dynamics, and lack a commonsense understanding of the environment, which limits their effectiveness. Our approach leverages Vision-Language Models (VLMs) to provide common sense scene understanding, such as recognizing traffic signs, crosswalks, and curbs for global navigation.

Language Foundation Models in Navigation: Recent breakthroughs in Language Foundation Models (LFMs) [5], encompassing VLMs and LLMs, demonstrate significant potential for robotic navigation. LM-Nav [36] employs GPT-3 and CLIP [31] to extract landmark descriptions from text-based navigation instruction and ground them in images, effectively guiding a robot to the goal in outdoor environments. VLMaps [18] propose a spatial map representation by fusing vision-language features with a 3D map that enables natural language-guided navigation. CoW [11] performs zero-shot language-based object navigation by combining CLIP-based maps and traditional exploration methods. Most of these researches focus on utilizing VLMs for high-level navigation guidance by extracting text-image scene representation. For low-level navigation behaviors, VLM-Social-Nav [40] explores the ability of VLM to extract socially compliant navigation behavior with the interaction with social entities like humans. CoNVOI [32] uses visual annotation to extract a sequence of waypoints from camera observation to navigate robots. PIVOT [28] uses visual prompting and optimization with VLMs in various low-level robot control tasks including indoor navigation. It shows the potential of a visual prompting approach for VLMs in robotic and spatial reasoning domains. Building on these approaches, our work uses VLMs to guide low-level navigation behavior by understanding contextual and semantic information about the surroundings. We use visual annotations [27, 28, 32, 38, 45], such as lines and numbers, to aid VLMs to effectively comprehend spatial information. Instead of randomly sampling the candidates

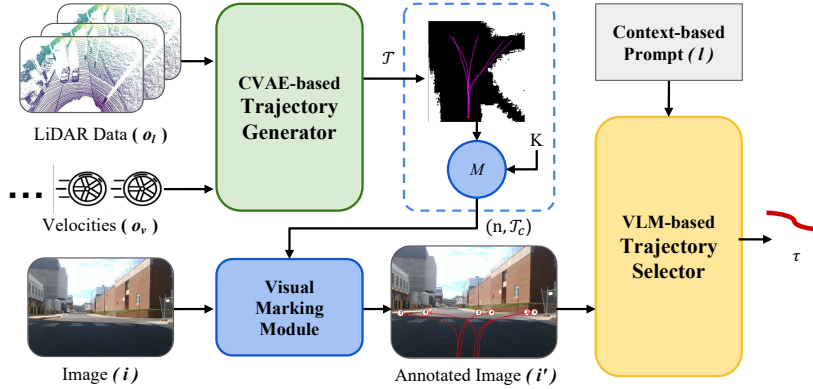


Fig. 2. Architecture: Our approach consists of two stages: CVAE-based trajectory generation and VLM-based trajectory selection. In the first stage, our attention-based CVAE takes consecutive frames of LiDAR point clouds and robot velocities as input, generating multiple diverse trajectories. These trajectories are resorted and visually marked with lines and numbers in the robot-view RGB image. In the second stage, our VLM-based trajectory selection module identifies the best trajectory number based on semantic feasibility, ensuring it lies on the sidewalk, avoids structures, crosses at zebra crossings, and adheres to other contextual rules.

like in PIVOT [28], we use a generative model-based trajectory generation approach to produce high-quality but diverse trajectories that ensure traversability for a VLM to choose from.

3 Approach

In this section, we formulate the problem of mapless global navigation and describe our approach.

3.1 Problem Formulation

Our approach computes a trajectory in a mapless environment for global navigation. To effectively leverage multi-modal sensor inputs, we design a two-stage pipeline, as shown in Figure 2, to select the best trajectory in terms of traversability and human-like decision making. Given a long-distance (e.g., 200m) goal $g \in \mathcal{O}_g$, we use a GPS sensor to provide the relative position between the target and the current location. We utilize both color and geometry modalities to generate a trajectory, τ , for global navigation. Our goal is to compute a trajectory, τ , that aims to provide the best path to the goal, prevent dead ends, and that satisfies the traversability constraints of the scenario, $\tau = TGS(\mathbf{l}, \mathbf{i}, \mathbf{o}, g)$, where $\mathbf{o} = \{\mathbf{o}_l, \mathbf{o}_v, \mathbf{i}\}$ represents the robot's observations. $\mathbf{o}_l \in \mathcal{O}_l$ represents LiDAR observations, $\mathbf{o}_v \in \mathcal{O}_v$ indicates the robot's velocity and $\mathbf{i} \in \mathcal{I}$ represents the RGB images from the camera. $\mathbf{l} = \{\mathbf{l}_t, \mathbf{l}_d\}$ represents the language instructions to the Vision-Language Models (VLMs) for acquiring traversable trajectories (\mathbf{l}_t) and the best direction (\mathbf{l}_d) to the goal, while avoiding dead ends.

We use Conditional Variational Autoencoder(CAVE) [22] to process the geometric information $\mathbf{o}_l \in \mathcal{O}_l$ from the LiDAR sensor and the consecutive velocities, $\mathbf{o}_v \in \mathcal{O}_v$, from the robot's odometer. We efficiently generate a set of trajectories lying in geometrically traversable areas, $\mathcal{T} = CVAE(\mathbf{o}_l, \mathbf{o}_v)$. These generated trajectories cannot handle geometrically similar but color-semantically different situations, such as crosswalks as shown in Figure 1 (C). Therefore, we use VLMs to provide scene understanding from the RGB images.

However, the generated real-world waypoints from CVAE and the image observations can have very different modalities. One way to fuse the two modalities is to overlay the trajectories on the images and use VLMs to analyze if the trajectories are in the traversable areas. We assume that VLMs can understand common sense from the images. Therefore, we use numbers to indicate the trajectories, where the numbers are computed using the distances between the last waypoints of the trajectories and the given target. We place these numbers at the end of each trajectory on the image to provide a better sense of sparse directions of the trajectories to the VLMs. Thus, we map the real-world trajectories to image pixel-level objects by

$$(\mathbf{n}, \mathcal{T}_c) = M(\mathcal{T}, K),$$

where K denotes the conversion matrix from the real-world LiDAR frame to the image plane, \mathcal{T}_c denotes the converted trajectories, and $\mathbf{n} \in \mathcal{N}$ are the numbers corresponding to each trajectory.

Given the language instruction $\mathbf{l}_t \in \mathcal{L}$ and the image $\mathbf{i} \in \mathcal{I}$ with the converted trajectories \mathcal{T}_c and numbers $\mathbf{n} \in \mathcal{N}$, VLM selects one traversable trajectory based on the color-semantic understanding of the scenarios, $\mathcal{T}_s = VLM(\mathbf{l}_t, \mathbf{i}, \mathcal{T}_c, \mathbf{n})$, where $\mathcal{T}_s \in \mathcal{A}$ and \mathcal{A} represents the ground truth traversable areas in the image \mathbf{i} . Furthermore, the selected trajectories are still not necessarily the best for navigation, so we use the \mathbf{l}_d language prompt to provide the goal direction and require VLMs to choose the traversable trajectory, \mathcal{T}_s , avoiding dead-ends and also satisfying social cues, such as lying on crosswalks and sidewalks. By combining \mathbf{l}_d and \mathbf{l}_t as \mathbf{l} , we choose the trajectory with the most probability as the human-decided trajectories, $\max P(\tau | \mathbf{l}, \mathbf{i}, \mathcal{T}_c, \mathbf{n})$. Therefore, the problem is defined as:

$$\max P(\tau | \mathbf{l}, \mathbf{i}, \mathcal{T}_c, \mathbf{n}), \text{ where } (\mathbf{n}, \mathcal{T}_c) = M(CAVE(\mathbf{o}_l, \mathbf{o}_v), K). \quad (1)$$

3.2 Geometry-based Trajectory Generation

The trajectory set, \mathcal{T} , is generated by a Conditional Variational Autoencoder (CVAE) to generate trajectories with associated confidences. For each observation $\{\mathbf{o}_l, \mathbf{o}_v\}$, we calculate the condition value $\mathbf{c} = f_e(\mathbf{o}_l, \mathbf{o}_v)$ for the CVAE decoder, where $f_e(\cdot)$ denotes the perception encoder. The embedding vector is then calculated from \mathbf{c} as $\mathbf{z} = f_z(\mathbf{c})$, with $f_z(\cdot)$ representing a neural network.

To compute enough candidates for robot's navigation, we need to generate multiple trajectories diverse enough to cover all traversable areas in front of

the robot. Since the decoder is designed to generate one trajectory with one embedding vector, generating multiple diverse trajectories requires representative and diverse embedding vectors. We project the embedding vector \mathbf{z} onto orthogonal axes by linear transformations, each projected vector corresponds to one traversable area. Then we generate trajectories based on the condition \mathbf{c} , as shown in Equation 2:

$$\mathbf{z}_k = A_k(c)\mathbf{z} + b_k(c) = h_{\psi_k}(\mathbf{z}), \quad (2)$$

where h_{ψ_k} denotes the linear transformation of \mathbf{z} . Using each embedding vector \mathbf{z}_k , the decoder generates a trajectory τ_k , as $p(\tau_k | \mathbf{z}_k^s, \mathbf{c}, \bar{\mathcal{Z}}_k)$. $\tau_k \in \mathcal{T}$ represents generated trajectories. \mathbf{z}_k and $\bar{\mathcal{Z}}_k$ are the embedding vectors of the current trajectory and the set of other trajectory embeddings, respectively. During training, \mathbf{z}_k is sampled from the projected distribution of the encoder output $h_{\psi_k}(f_z(\mathbf{c}))$. Each waypoint of \mathbf{z}_k . The training of the trajectory generator is the same as [22], where we use traversability loss, CVAE lower bound, and diversity loss to train the model.

3.3 VLM-based Trajectory Selection

Algorithm 1 highlights our procedure of using VLMs to select a suitable trajectory from candidate trajectories. The generated trajectories \mathcal{T} are obtained from the latest consecutive $t = 2$ time steps. Given the collected trajectories in \mathcal{T} , we convert them to the image plane with numbers, where we sort the trajectories in terms of heuristic, which is the distance between the last waypoint of the trajectory and the goal: $(\mathbf{n}, \mathcal{T}_c) = M(\mathcal{T}, K, T_c)$, where T_c denotes the extrinsic transformation between the camera frame and the robot's frame to convert the trajectories from the robot's frame to the image plane.

Considering that the trajectories generated from consecutive time steps can be very close to each other, we only select representative trajectories from $\mathcal{T}' \subseteq \mathcal{T}$ based on the Hausdorff distances among all the trajectories:

$$\forall \tau_n, \tau_m \in \mathcal{T}', d_h(\tau_n, \tau_m) > d_t, \text{ where } n \neq m, \quad (3)$$

where $d_h(\cdot, \cdot)$ represents the Hausdorff distance and d_t denotes the distance threshold.

We then project the trajectories \mathcal{T}' from the robot's frame to the camera frame, $\mathcal{T}_r = P_t(\mathcal{T}', T_c)$. The trajectories are subsequently projected into the camera image plane $\mathcal{T}'_c = P_c(\mathcal{T}_r, K)$, where the K is the intrinsic matrix of the camera. Following the trajectory generation sequence, we annotate the trajectories with numbers, \mathbf{n} .

Finally, we use Vision-Language Models (VLMs) to select the best trajectory in terms of satisfying traversability, on crosswalks to satisfy social compliance and avoiding dead-ends. The annotated trajectories $(\mathbf{n}, \mathcal{T}_c)$ and the current observation image \mathbf{i} are input into the VLMs with the prompt instruction \mathbf{l} . VLMs select the best trajectory, τ , in terms of traversability, social compliance, and the traveling distance to the goal:

$$\tau = \text{VLMs}(\mathbf{l}, \mathbf{i}, \mathcal{T}_c, \mathbf{n}). \quad (4)$$

The example prompt instruction **I** is as follows:

Pick one path that I should follow to navigate safely, like what humans do. Remember that I must walk on pavements, avoid rough, bumpy terrains, and follow the rules. I cannot go over/under the curbs. The lower number indicates the shortest path to the goal. Pick only one. Provide the answer in this form: {'trajectory': []}

Algorithm 1 Multi-modal Mapless Global Navigation: d_t denotes the threshold of Hausdorff distances among the trajectories. The new trajectories generated by CVAE are represented as \mathcal{T}_n , while the historic trajectories are indicated as \mathcal{T}_h . \mathbf{a} denotes actions generated from motion planner given τ .

Require: $t \leftarrow 2$, g , and **I**.
Require: $\mathcal{T} = \{\}$

```

while the robot is running do
     $\mathcal{T}_n = CVAE(\mathbf{o}_l, \mathbf{o}_v)$ 
     $\mathcal{T} = \mathcal{T}_n \cup \mathcal{T}$ 
     $(\mathbf{n}, \mathcal{T}_c) = M(\mathcal{T}, K, T_c, d_t)$ 
     $\tau = VLMs(\mathbf{l}, \mathbf{i}, \mathcal{T}_c, \mathbf{n})$ 
     $\mathbf{a} = \text{Motion Planner}(\tau)$ 
    if  $|\mathcal{T}| > t$  then
         $\mathcal{T}.\text{POP}(0)$ 
    end if
end while

```

4 Experimental Results

In this section, we present the details of the implementation, qualitative results, quantitative results, and ablation studies of our approach.

4.1 Implementation Details

Our approach is tested on a Clearpath Husky equipped with a Velodyne VLP16 LiDAR, a Realsense D435i, and a laptop with Intel i7 CPU and an Nvidia GeForce RTX 2080 GPU. We use CVAE [22] with an attention mechanism to generate multiple trajectories (approximately 15m each), and use GPT-4V [1] as VLM to select the best traversable trajectory.

The training dataset for our CVAE-based trajectory generation model contains three parts: 1) LiDAR point cloud and robot velocities, 2) binary traversability maps only for training and evaluations, shown in the bottom row of Fig. 4 and Fig. 5, and 3) randomly generated diverse targets and the shortest ground truth trajectories to the targets.

To validate TGS, we present qualitative and quantitative results compared with MTG [22], ViNT [37], NoMaD [41], and CoNVOI [32]. MTG selects the trajectory with the shortest distance between the last waypoint and the goal. For evaluation, we randomly select the target goal for MTG and TGS within

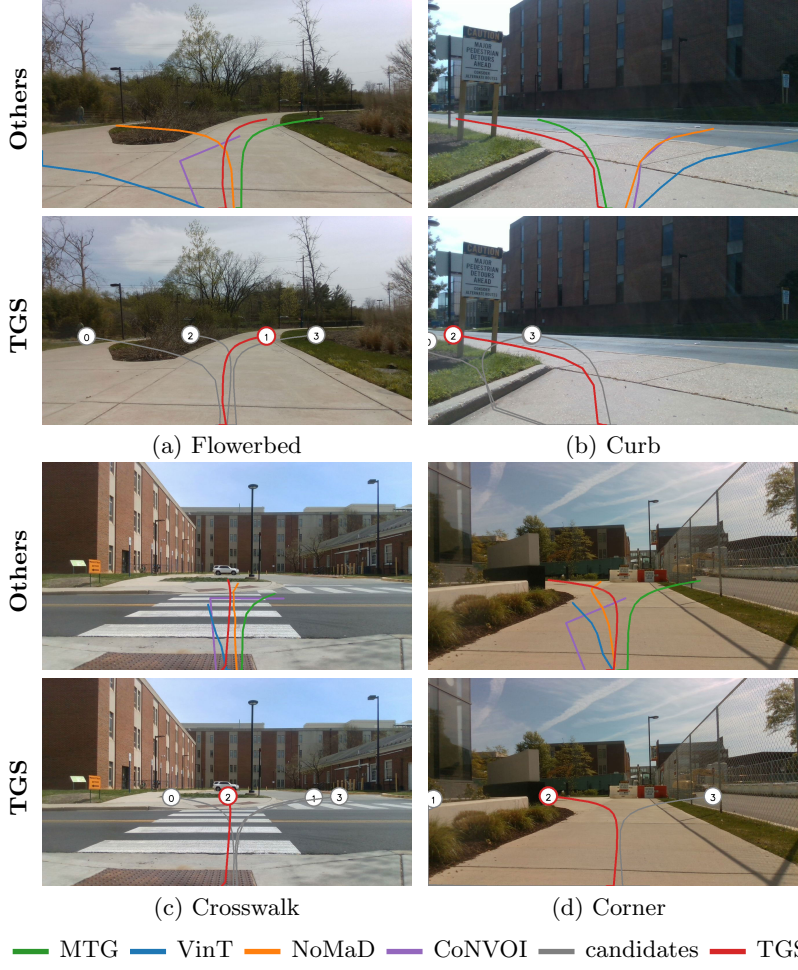


Fig. 3. Qualitative Results: The top row shows the generated trajectories using all the methods, MTG [22] in green, ViNT [37] in blue, NoMaD [41] in orange, CoNVOI [32] in purple, and TGS in red. The bottom row shows the candidate trajectories in gray marked with numbers and the selected trajectory in red using TGS. TGS can generate and select a long-range trajectory that is both geometrically and semantically feasible.

50m of the current position. ViNT, NoMaD, and CoNVOI use topological nodes to navigate robot and do not consider optimality to the goal. MTG uses only LiDAR data, ViNT and NoMaD rely solely on RGB images. CoNVOI is similar to our approach and uses LiDAR to mark numbers in the RGB images for VLM input. We evaluate the performance in four challenging benchmark scenarios:

- **Flower bed:** A robot navigating a paved area next to a flower bed. The robot must stay on the paved path and avoid entering the flower bed. An open flower bed consisting of short grass is difficult to detect with a LiDAR.
- **Curb:** A robot navigating in a sidewalk, which is distinctly separated from the roadway by a curb. The robot must stay on a sidewalk or select a

traversable trajectory to go around curbs. As both the sidewalk and the roadway can be considered traversable for the wheel robots, it is challenging to select the traversable trajectory around curbs.

- **Crosswalk:** A robot crossing the zebra crossing. The robot must stay on the crosswalk when crossing the street. It is difficult to tell the difference between the crosswalk and the driveway.
- **Around the corner:** The straight line to the target leads to a dead-ends and a robot needs to choose trajectories deviates from the direction of the target temporarily. It is hard to avoid such a dead end without understanding the spatial context of the environment.

4.2 Qualitative Results

Figure 3 shows the resulting robot trajectories corresponding to four different approaches in four different scenarios. The upper row shows the trajectories generated by all the comparison methods including ours and the lower row shows the results of TGS with the candidate trajectories (grey) and the selected one. We demonstrate that our method can generate and select a long-range trajectory that satisfy various constraints.

ViNT [37] and NoMaD [41] compare current observation with pre-recorded subgoal images and choose the most similar one as the next waypoint. These methods are successful in terms of following a straight path with prominent visual features, especially in crosswalk scenarios. However, these methods often struggle to generate feasible trajectories in scenarios with turns. The accuracy decreases significantly in cases involving substantial scene changes. MTG with heuristic selects the trajectory closest to the target goal, which often leads to paths that may not follow the sidewalks and crosswalks. In corner cases where the target goal is located around a bend or behind a structure, MTG tends to fail by attempting to cut through rather than effectively navigating around the structure. Although CoNVOI generates feasible trajectories, they are zigzag leading to non-smooth robot actions. As shown in the bottom row of each scenario in Fig. 3, our approach produces diverse trajectories and selects the best one traversable, socially compliant and avoiding dead-ends.

4.3 Quantitative Results

To further validate TGS, we evaluate the methods using two different metrics:

- **Traversability:** The ratio of the generated trajectory lying on a traversable area. This metric is calculated as

$$tr(\mathcal{A}, \hat{\tau}) = \bigcap_{m=1}^M c(\mathcal{A}, \mathbf{w}_m), \quad \mathbf{w}_m \in \hat{\tau}. \quad (5)$$

where $c(\cdot)$ tells if the waypoint \mathbf{w}_m is in the traversable area \mathcal{A} .

- **Fréchet Distance w.r.t. Human Teleoperation:** Fréchet Distance [3] is one of the measures of similarity between two curves. We measure the similarity between the trajectory generated and selected by the methods and a human-teleoperated trajectory. A lower distance indicates a higher degree of similarity.

Table 1 reports the results averaged over 100 frames for each method and scenario. The results demonstrate that TGS outperforms other SOTA approaches in most of the cases. Specifically, we achieve at least 3.35% and at most 47.74% improvement in terms of average traversability, and at least 20.61% and at most 40.98% improvement in terms of average Fréchet distance. Overall, the average improvement rates are approximately 22.07% for traversability and 30.53% in the Fréchet distance. CoNVOI achieved comparable results in terms of traversability. However, this is because CoNVOI calculates relatively short trajectories, which means the waypoints are much less likely to fall within non-traversable areas. We observe that because CoNVOI only considers the traversability of the two waypoints and not the points that linearly connect those two selected points, the intermediate points often lie in non-traversable areas. We also observe that MTG produced very low results in terms of traversability. This was not only because our benchmark scenarios were selected based on scenarios that are difficult to detect with LiDAR, but also because MTG often failed to consider traversability while focusing on optimality to the goal. In terms of Fréchet distance, MTG and TGS produce good results because they output trajectories similar in length to the 15m-long human-operated trajectory we compared against. In contrast, CoNVOI generated a linear trajectory that differs significantly from typical human-operated trajectories, resulting in a lower similarity.

Table 1. Quantitative Results: Comparisons with MTG [22], ViNT [37], NoMaD [41], and CoNVOI [32] in terms of traversability and human-like navigation similarity. TGS achieves at least 3.35% improvement in the traversability and 20.61% improvement in Fréchet distance. In the Input column, L indicates the LiDAR point cloud and I indicates the RGB images.

Metric	Method	Input	Scenario			
			Flower bed	Curb	Crosswalk	Corner
Traversability (%)	MTG	L	58.19	67.12	61.82	44.71
	ViNT	I	63.62	78.37	84.78	44.95
	NoMaD	I	75.64	83.13	79.24	77.38
	CoNVOI	L+I	81.10	75.68	86.24	88.46
	TGS	L+I	87.22	89.93	87.44	78.00
Fréchet Distance (m)	MTG	L	6.61	8.40	10.42	9.93
	ViNT	I	10.43	10.78	11.87	12.71
	NoMaD	I	7.65	8.71	8.94	9.62
	CoNVOI	L+I	11.64	12.24	11.33	12.36
	TGS	L+I	5.27	7.93	6.38	8.49

4.4 Ablation Study

To evaluate the capability of different components of our innovations, we compare TGS with two different settings. First, we compare with *MTG only*, with heuristic to select the shortest travel distance to the goal. This comparison shows how our visual markings and VLM can handle more diverse and challenging scenarios that require context information from the surrounding environment.

Second, we compare with *VLM with visual annotation only* [28], with a random sampling method to generate trajectory. This comparison shows how giving a nice set of candidates to VLM could benefit our approach.

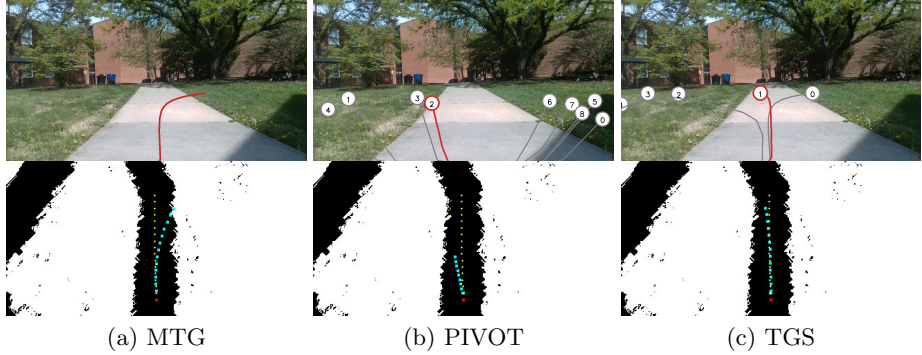


Fig. 4. Ablation Studies Results: Comparisons with (a) MTG , (b) PIVOT with randomly sampled candidate trajectories, and (c) TGS. The top row shows the generated candidate trajectories (gray) and the selected trajectory (red) in the robot-view image. The bottom row shows the top-down view image of the traversability map. The cyan color represents the generated trajectories from the three methods, and the yellow color represents the human-driven trajectory. Compared with other approaches, TGS selects the trajectory closest to the human-driven one, which keeps the robot in the center of the pavement.

As shown in Fig. 4 and Fig. 3, when comparing MTG and TGS , MTG fails to consider traversability that is hard to detect from LiDAR. Flower beds with short grass, curbs, and crosswalks are such scenarios. TGS uses both the geometric information obtained from LiDAR to generate multiple candidate trajectories and the semantic information obtained from the image and selects a feasible trajectory. Especially because MTG selects the trajectory with heuristic, a distance to the goal, it often results in the trajectories that go over the grass or curbs. This shows how the visual prompting method can help make human-level decisions on trajectory selection. Instead of generating candidate trajectories using the CVAE-based trajectory generation method, Fig. 4(c) illustrates randomly sampled candidate trajectories, a visual prompting method explored by PIVOT [28]. We randomly sampled waypoints that are within 5m to 15m ahead and then linearly connected the points to generate trajectories. Unlike PIVOT approach, we did not apply the iterative questioning method, which was not applicable to our real-time navigation pipeline, but instead generated 10 random points. While this approach can select the best trajectory from the provided candidate trajectories, it does not yield the optimal trajectory in terms of similarity to the human-operated trajectory when compared to TGS. This highlights the importance of trajectory generation, providing high-quality candidates to the VLMs.

Figure 5 illustrates different visual marking approaches. The red lines and numbers are the marks given as input to VLM. The green line indicates the se-

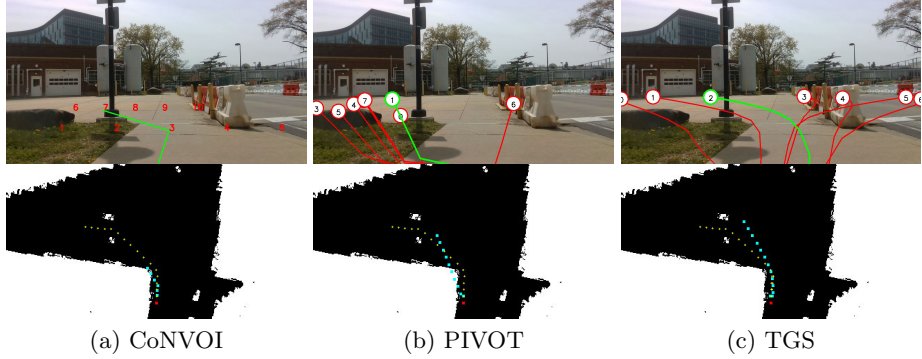


Fig. 5. Different Visual Marking Methods: The top row shows the visually annotated image with the red lines and numbers, which is the input provided to VLMs. The green line indicates the selected trajectory. The bottom row shows the top-down view image of the traversability map. The cyan color represents the generated trajectories, and the yellow color represents the human-driven trajectory. Compared with other approaches, TGS selects the trajectory smoother and longer than CoNVOI and with better traversability than PIVOT.

lected trajectory by VLM. CoNVOI uses numbers to mark obstacle-free regions and selects numbers to navigate. Although the marked regions can be obstacle-free, it does not consider the waypoints in between. This can result in going through the obstacle. PIVOT randomly generates the sub-goal target and linearly connects them. Because the target is randomly generated, it often fails to generate nice candidates. TGS combines the strengths of both approaches. While the CVAE-based trajectory generation produces diverse trajectories, it utilizes visual prompting with lines and numbers to assist the VLM’s spatial reasoning, ultimately selecting the most feasible trajectory.

5 Conclusion, Limitations, and Future Work

We propose TGS, a novel multi-modal Trajectory Generation and Selection approach for mapless outdoor navigation. TGS integrates a CVAE-based trajectory generation method with a VLM-based trajectory selection process to compute geometrically and semantically feasible trajectories in challenging outdoor environments. Our approach achieves at least a 3.35% improvement in traversability and a 20.61% improvement in similarity to human-operated trajectories.

Our method has a few limitations. Since TGS relies on VLMs, its performance can depend on the robustness of the VLM. However, as VLMs continue to improve, which is currently happening, the robustness of our approach can also be enhanced. Additionally, our trajectory generation method can be replaced by better approaches at any time, potentially leading to further performance improvements. We need to evaluate its performance in more complex environments.

References

1. Achiam, J., Adler, S., Agarwal, S., Ahmad, L., Akkaya, I., Aleman, F.L., Almeida, D., Altenschmidt, J., Altman, S., Anadkat, S., et al.: Gpt-4 technical report. arXiv preprint arXiv:2303.08774 (2023)
2. Alayrac, J.B., Donahue, J., Luc, P., Miech, A., Barr, I., Hasson, Y., Lenc, K., Mensch, A., Millican, K., Reynolds, M., et al.: Flamingo: a visual language model for few-shot learning. Advances in neural information processing systems **35** (2022) 23716–23736
3. Alt, H., Godau, M.: Computing the fréchet distance between two polygonal curves. International Journal of Computational Geometry & Applications **5**(01n02) (1995) 75–91
4. Austin, J., Odena, A., Nye, M., Bosma, M., Michalewski, H., Dohan, D., Jiang, E., Cai, C., Terry, M., Le, Q., et al.: Program synthesis with large language models. arXiv preprint arXiv:2108.07732 (2021)
5. Bommashani, R., Hudson, D.A., Adeli, E., Altman, R., Arora, S., von Arx, S., Bernstein, M.S., Bohg, J., Bosselut, A., Brunskill, E., et al.: On the opportunities and risks of foundation models. arXiv preprint arXiv:2108.07258 (2022)
6. Borges, P.V., Peynot, T., Liang, S., Arain, B., Wildie, M., Minareci, M., Lichman, S., Samvedi, G., Sa, I., Hudson, N., et al.: A survey on terrain traversability analysis for autonomous ground vehicles: Methods, sensors, and challenges. Field Robotics **2**(1) (2022) 1567–1627
7. Brown, T., Mann, B., Ryder, N., Subbiah, M., Kaplan, J.D., Dhariwal, P., Neelakantan, A., Shyam, P., Sastry, G., Askell, A., et al.: Language models are few-shot learners. Advances in neural information processing systems **33** (2020) 1877–1901
8. Chung, C., Georgakis, G., Spieler, P., Padgett, C., Agha, A., Khattak, S.: Pixel to elevation: Learning to predict elevation maps at long range using images for autonomous offroad navigation. IEEE Robotics and Automation Letters (2024)
9. Eom, W., Park, J., Lee, J.: Hazardous area navigation with temporary beacons. International Journal of Control, Automation and Systems **8**(5) (2010) 1082–1090
10. Fankhauser, P., Bloesch, M., Hutter, M.: Probabilistic terrain mapping for mobile robots with uncertain localization. IEEE Robotics and Automation Letters (RA-L) **3**(4) (2018) 3019–3026
11. Gadre, S.Y., Wortsman, M., Ilharco, G., Schmidt, L., Song, S.: Clip on wheels: Zero-shot object navigation as object localization and exploration. arXiv preprint arXiv:2203.10421 **3**(4) (2022) 7
12. Ganesan, S., Natarajan, S.K., Srinivasan, J.: A global path planning algorithm for mobile robot in cluttered environments with an improved initial cost solution and convergence rate. Arabian Journal for Science and Engineering **47**(3) (2022) 3633–3647
13. Gao, P., Liu, Z., Wu, Z., Wang, D.: A global path planning algorithm for robots using reinforcement learning. In: 2019 IEEE International Conference on Robotics and Biomimetics (ROBIO), IEEE (2019) 1693–1698
14. Giovannangeli, C., Gaussier, P., Désilles, G.: Robust mapless outdoor vision-based navigation. In: 2006 IEEE/RSJ international conference on intelligent robots and systems, IEEE (2006) 3293–3300
15. Gupta, A., Johnson, J., Fei-Fei, L., Savarese, S., Alahi, A.: Social gan: Socially acceptable trajectories with generative adversarial networks. In: Proceedings of the IEEE conference on computer vision and pattern recognition. (2018) 2255–2264

16. Ha, H., Song, S.: Semantic abstraction: Open-world 3d scene understanding from 2d vision-language models. arXiv preprint arXiv:2207.11514 (2022)
17. Hao, J., Yang, T., Tang, H., Bai, C., Liu, J., Meng, Z., Liu, P., Wang, Z.: Exploration in deep reinforcement learning: From single-agent to multiagent domain. *IEEE Transactions on Neural Networks and Learning Systems* (2023)
18. Huang, C., Mees, O., Zeng, A., Burgard, W.: Visual language maps for robot navigation. In: 2023 IEEE International Conference on Robotics and Automation (ICRA), IEEE (2023) 10608–10615
19. Jeong, I., Jang, Y., Park, J., Cho, Y.K.: Motion planning of mobile robots for autonomous navigation on uneven ground surfaces. *Journal of Computing in Civil Engineering* **35**(3) (2021) 04021001
20. Kim, D., Sun, J., Oh, S.M., Rehg, J.M., Bobick, A.F.: Traversability classification using unsupervised on-line visual learning for outdoor robot navigation. In: Proceedings 2006 IEEE International Conference on Robotics and Automation, 2006. ICRA 2006., IEEE (2006) 518–525
21. Kirillov, A., Mintun, E., Ravi, N., Mao, H., Rolland, C., Gustafson, L., Xiao, T., Whitehead, S., Berg, A.C., Lo, W.Y., et al.: Segment anything. In: Proceedings of the IEEE/CVF International Conference on Computer Vision. (2023) 4015–4026
22. Liang, J., Gao, P., Xiao, X., Sathyamoorthy, A.J., Elnoor, M., Lin, M., Manocha, D.: Mtg: Mapless trajectory generator with traversability coverage for outdoor navigation. arXiv preprint arXiv:2309.08214 (2023)
23. Liang, J., Patel, U., Sathyamoorthy, A.J., Manocha, D.: Crowd-steer: Realtime smooth and collision-free robot navigation in densely crowded scenarios trained using high-fidelity simulation. In: Proceedings of the Twenty-Ninth International Conference on International Joint Conferences on Artificial Intelligence. (2021) 4221–4228
24. Liang, J., Payandeh, A., Song, D., Xiao, X., Manocha, D.: Dtg: Diffusion-based trajectory generation for mapless global navigation. arXiv preprint arXiv:2403.09900 (2024)
25. Liang, J., Qiao, Y.L., Guan, T., Manocha, D.: Of-vo: Efficient navigation among pedestrians using commodity sensors. *IEEE Robotics and Automation Letters* **6**(4) (2021) 6148–6155
26. Liang, J., Weerakoon, K., Guan, T., Karapetyan, N., Manocha, D.: Adaptiveon: Adaptive outdoor local navigation method for stable and reliable actions. *IEEE Robotics and Automation Letters* **8**(2) (2022) 648–655
27. Liu, F., Fang, K., Abbeel, P., Levine, S.: Moka: Open-vocabulary robotic manipulation through mark-based visual prompting. arXiv preprint arXiv:2403.03174 (2024)
28. Nasiriany, S., Xia, F., Yu, W., Xiao, T., Liang, J., Dasgupta, I., Xie, A., Driess, D., Wahid, A., Xu, Z., et al.: Pivot: Iterative visual prompting elicits actionable knowledge for vlms. arXiv preprint arXiv:2402.07872 (2024)
29. Ort, T., Gilitschenski, I., Rus, D.: Autonomous navigation in inclement weather based on a localizing ground penetrating radar. *IEEE Robotics and Automation Letters* **5**(2) (2020) 3267–3274
30. Psotka, M., Duchon, F., Roman, M., Michal, T., Michal, D.: Global path planning method based on a modification of the wavefront algorithm for ground mobile robots. *Robotics* **12**(1) (2023) 25
31. Radford, A., Kim, J.W., Hallacy, C., Ramesh, A., Goh, G., Agarwal, S., Sastry, G., Askell, A., Mishkin, P., Clark, J., et al.: Learning transferable visual models from natural language supervision. In: International conference on machine learning, PMLR (2021) 8748–8763

32. Sathyamoorthy, A.J., Weerakoon, K., Elnoor, M., Zore, A., Ichter, B., Xia, F., Tan, J., Yu, W., Manocha, D.: Convoi: Context-aware navigation using vision language models in outdoor and indoor environments. arXiv preprint arXiv:2403.15637 (2024)
33. Schmid, L., Pantic, M., Khanna, R., Ott, L., Siegwart, R., Nieto, J.: An efficient sampling-based method for online informative path planning in unknown environments. IEEE Robotics and Automation Letters **5**(2) (2020) 1500–1507
34. Shafiee, M.J., Chywl, B., Li, F., Wong, A.: Fast yolo: A fast you only look once system for real-time embedded object detection in video. arXiv preprint arXiv:1709.05943 (2017)
35. Shah, D., Levine, S.: Viking: Vision-based kilometer-scale navigation with geographic hints. arXiv preprint arXiv:2202.11271 (2022)
36. Shah, D., Osiński, B., Levine, S., et al.: Lm-nav: Robotic navigation with large pre-trained models of language, vision, and action. In: Conference on robot learning, PMLR (2023) 492–504
37. Shah, D., Sridhar, A., Dashora, N., Stachowicz, K., Black, K., Hirose, N., Levine, S.: Vint: A foundation model for visual navigation. arXiv preprint arXiv:2306.14846 (2023)
38. Shtedritski, A., Rupprecht, C., Vedaldi, A.: What does clip know about a red circle? visual prompt engineering for vlms. In: Proceedings of the IEEE/CVF International Conference on Computer Vision. (2023) 11987–11997
39. Sohn, K., Lee, H., Yan, X.: Learning structured output representation using deep conditional generative models. Advances in neural information processing systems **28** (2015)
40. Song, D., Liang, J., Payandeh, A., Xiao, X., Manocha, D.: Socially aware robot navigation through scoring using vision-language models. arXiv preprint arXiv:2404.00210 (2024)
41. Sridhar, A., Shah, D., Glossop, C., Levine, S.: Nomad: Goal masked diffusion policies for navigation and exploration. arXiv preprint arXiv:2310.07896 (2023)
42. Weerakoon, K., Sathyamoorthy, A.J., Liang, J., Guan, T., Patel, U., Manocha, D.: Graspe: Graph based multimodal fusion for robot navigation in outdoor environments. IEEE Robotics and Automation Letters (2023)
43. Wijayathunga, L., Rassau, A., Chai, D.: Challenges and solutions for autonomous ground robot scene understanding and navigation in unstructured outdoor environments: A review. Applied Sciences **13**(17) (2023) 9877
44. Wu, T., He, S., Liu, J., Sun, S., Liu, K., Han, Q.L., Tang, Y.: A brief overview of chatgpt: The history, status quo and potential future development. IEEE/CAA Journal of Automatica Sinica **10**(5) (2023) 1122–1136
45. Yang, J., Zhang, H., Li, F., Zou, X., Li, C., Gao, J.: Set-of-mark prompting unleashes extraordinary visual grounding in gpt-4v. arXiv preprint arXiv:2310.11441 (2023)
46. Zhai, H., Egerstedt, M., Zhou, H.: Path exploration in unknown environments using fokker-planck equation on graph. Journal of Intelligent & Robotic Systems **104**(4) (2022) 71
47. Zhang, J., Yang, K., Constantinescu, A., Peng, K., Müller, K., Stiefelhagen, R.: Trans4trans: Efficient transformer for transparent object and semantic scene segmentation in real-world navigation assistance. IEEE Transactions on Intelligent Transportation Systems **23**(10) (2022) 19173–19186
48. Zhang, Y., Ge, R., Lyu, L., Zhang, J., Lyu, C., Yang, X.: A virtual end-to-end learning system for robot navigation based on temporal dependencies. IEEE Access **8** (2020) 134111–134123